



Article

Gut Region-Specific Interleukin 1 β Induction in Different Myenteric Neuronal Subpopulations of Type 1 Diabetic Rats

Afnan AL Doghmi , Bence Pál Barta , Abigél Egyed-Kolumbán, Benita Onhausz, Szilvia Kiss, János Balázs, Zita Szalai, Mária Bagyánszki and Nikolett Bódi *

Department of Physiology, Anatomy and Neuroscience, University of Szeged, 6726 Szeged, Hungary

* Correspondence: bodi.nikolett@bio.u-szeged.hu

Abstract: Interleukin 1 β (IL1 β) is a pro-inflammatory cytokine that may play a crucial role in enteric neuroinflammation in type 1 diabetes. Therefore, our goal is to evaluate the effects of chronic hyperglycemia and insulin treatment on IL1 β immunoreactivity in myenteric neurons and their different subpopulations along the duodenum–ileum–colon axis. Fluorescent immunohistochemistry was used to count IL1 β expressing neurons as well as the neuronal nitric oxide synthase (nNOS)- and calcitonin gene-related peptide (CGRP)-immunoreactive myenteric neurons within this group. Tissue IL1 β level was measured by ELISA in muscle/myenteric plexus-containing homogenates. IL1 β mRNA was detected by RNAscope in different intestinal layers. The proportion of IL1 β -immunoreactive myenteric neurons was significantly higher in the colon than in the small intestine of controls. In diabetics, this proportion significantly increased in all gut segments, which was prevented by insulin treatment. The proportion of IL1 β -nNOS-immunoreactive neurons only increased in the diabetic colon, while the proportion of IL1 β -CGRP-immunoreactive neurons only increased in the diabetic ileum. Elevated IL1 β levels were also confirmed in tissue homogenates. IL1 β mRNA induction was detected in the myenteric ganglia, smooth muscle and intestinal mucosa of diabetics. These findings support that diabetes-related IL1 β induction is specific for the different myenteric neuronal subpopulations, which may contribute to diabetic motility disturbances.

Keywords: interleukin 1 β enteric nervous system; myenteric neurons; neuronal nitric oxide synthase; calcitonin gene-related peptide; type 1 diabetes; hyperglycemia; insulin; gut regions



Citation: AL Doghmi, A.; Barta, B.P.; Egyed-Kolumbán, A.; Onhausz, B.; Kiss, S.; Balázs, J.; Szalai, Z.; Bagyánszki, M.; Bódi, N. Gut Region-Specific Interleukin 1 β Induction in Different Myenteric Neuronal Subpopulations of Type 1 Diabetic Rats. *Int. J. Mol. Sci.* **2023**, *24*, 5804. <https://doi.org/10.3390/ijms24065804>

Academic Editors: Maria Addolorata Bonifacio and Maria A. Mariggiò

Received: 26 February 2023
Revised: 13 March 2023
Accepted: 16 March 2023
Published: 18 March 2023



Copyright: © 2023 by the authors. Licensee MDPI, Basel, Switzerland. This article is an open access article distributed under the terms and conditions of the Creative Commons Attribution (CC BY) license (<https://creativecommons.org/licenses/by/4.0/>).

1. Introduction

Inflammatory cytokines, such as tumor necrosis factor alpha (TNF α) or different interleukins (ILs), trigger chronic low-grade inflammation that is linked to the development and progression of type 1 diabetes [1]. Due to the regionality of the intestinal structure and function, the regional cellular environment that accompanies diabetic gastroenteropathy has received special attention over the last decade [2–4]. Among others, the enteric neuronal microenvironment plays a pivotal role in the disturbed regulation of gut motility in diabetic patients [5–7]. However, the microbial environment of the intestinal epithelium, mucosal, submucosal and muscular milieu is also essential to the cellular crosstalk vertically in the gut wall [8].

Cytokines have global impacts on intestinal health and disease [9–12]. It has recently been shown that chronic hyperglycemia has regionally different effects on TNF α expression in distinct gut segments [13]. Moreover, the expression of TNF α receptors is also differently altered in the different segments; TNF receptor 2 is more affected than TNF receptor 1 in the duodenal myenteric ganglia of type 1 diabetic rats [14].

The IL1-family of cytokines consists of 11 members and is produced primarily by the vast majority of immune cells in response to microbial stimuli or other cytokines [15]. Among them, IL1 has two distinct isoforms, IL1 α and IL1 β , with only 26% homology

between them. Pro-IL1 β is functionally inactive; its cleavage is mediated by caspase-1 in inflammasomes, and then as a bioactive pro-inflammatory mediator it amplifies inflammatory cascades and regulates innate immunity [15–17]. IL1 has roles both in autoimmune and autoinflammatory diseases [18–20].

IL1 β promotes both systemic and tissue inflammation in diabetes, including β -cell apoptosis of pancreatic islets and diabetic cardiovascular complications related to increased IL1 β expression in the aorta endothelium, heart and retinal vessels of diabetic rats [21,22]. IL1 β and other pro-inflammatory cytokines are also elevated in inflammatory bowel disease and necrotizing enterocolitis, inducing intestinal inflammation through the disruption of the epithelial junctional barrier [23]. IL1 β also serves as a key factor in the development and maintenance of neuropathic pain in different chronic states by mediating neuro-immune interactions in the spinal cord and brain [24]. However, so far only a few studies have focused on the role that IL1 β plays in the enteric nervous system [25–27].

Diabetic enteric neuropathy has been studied extensively [28,29], especially as the vast majority of diabetic patients suffer from gastrointestinal symptoms such as nausea, vomiting, diarrhea or constipation. In the background of these diabetic motility disturbances, the nitrergic myenteric subpopulation is particularly affected [5,30,31]. Nitrergic myenteric neurons (containing neuronal nitric oxide synthase, nNOS) represent a robust neuronal population in the myenteric plexus [32,33]. Most of these cells are inhibitory interneurons or motor neurons that are responsible for the descending inhibition of gut motility. However, nNOS neurons also have an important role in the inflammatory responses of enteric neurons in traumatic nerve injury, inflammatory bowel diseases or ischaemic damage [34–36]. On the other hand, intrinsic primary afferent neurons (IPANs), as transducers, are responsible for the detection of mechanical and chemical stimuli and for the initiation of enteric reflexes in the gut wall [37], therefore, their involvement is also crucial in peristalsis and other gut functions during diabetes. IPANs are characterized by Dogiel type II morphology and many of them contain calcitonin gene-related peptide (CGRP) [37,38] which is affected in diabetes [39].

Different subpopulations of myenteric neurons respond differently to diabetic damage [31,40,41]. Therefore, we presumed that inflammatory responses of these neuronal populations may also contain differences. The primary goal of this study was to evaluate the effects of chronic hyperglycemia and immediate insulin treatment on the proportion of IL1 β -immunoreactive (IR) myenteric neurons along the duodenum–ileum–colon axis. Moreover, we aimed to reveal whether a neuronal population-specific IL1 β immunoreactivity exists in the nNOS-IR and CGRP-IR subpopulations in type 1 diabetic rats.

2. Results

2.1. Weight and Glycemic Characteristics of Experimental Rats

The weight and blood glucose concentration of the diabetic, insulin-treated diabetic and control rats were monitored during the 10-week experiment and are summarized in Table 1.

Table 1. Weight and glycaemic characteristics of the experimental animals.

	Weight (g)		Blood Glucose Level (mmol/L)	
	Initial	Final	Initial	Final (Average)
Controls (n = 16)	206 \pm 2.48	445.6 \pm 13.58 ^c	4.82 \pm 0.29	5.81 \pm 0.1
Diabetics (n = 15)	206.1 \pm 2.57	317.7 \pm 13.34 ^{a,e}	5.47 \pm 0.42	27.05 \pm 1.12 ^{c,e}
Insulin-treated diabetics (n = 14)	216.1 \pm 5.37	432.1 \pm 15.12 ^{c,g}	5.21 \pm 0.42	12.57 \pm 1.19 ^{b,d,f}

Data are expressed as mean \pm SEM; ^a $p < 0.05$, ^b $p < 0.001$, ^c $p < 0.0001$ vs. initial; ^d $p < 0.01$, ^e $p < 0.0001$ vs. final controls; ^f $p < 0.05$, ^g $p < 0.001$ vs. final diabetics.

Diabetic rats were characterized by a long-lasting chronic hyperglycemia, their average blood glucose concentration was 27.05 ± 1.12 mmol/L, which was more than four times higher than that of the controls (5.81 ± 0.1 mmol/L). Immediate insulin treatment inhibited extremely high glucose levels, however, these were still higher than in the control group (12.57 ± 1.19 mmol/L). All the experimental rats gained weight during the 10-week experimental period, although the final body weight of diabetic animals was significantly lower compared to the insulin-treated diabetic ($p < 0.001$) and control ($p < 0.0001$) rats.

2.2. Gut Region-Specific Presence and Diabetic Induction of IL1 β -Immunoreactive Myenteric Neurons

Double-labelling fluorescent immunohistochemistry revealed regional differences in IL1 β immunoreactivity in myenteric neurons along the intestinal tract in control animals (Figure 1).

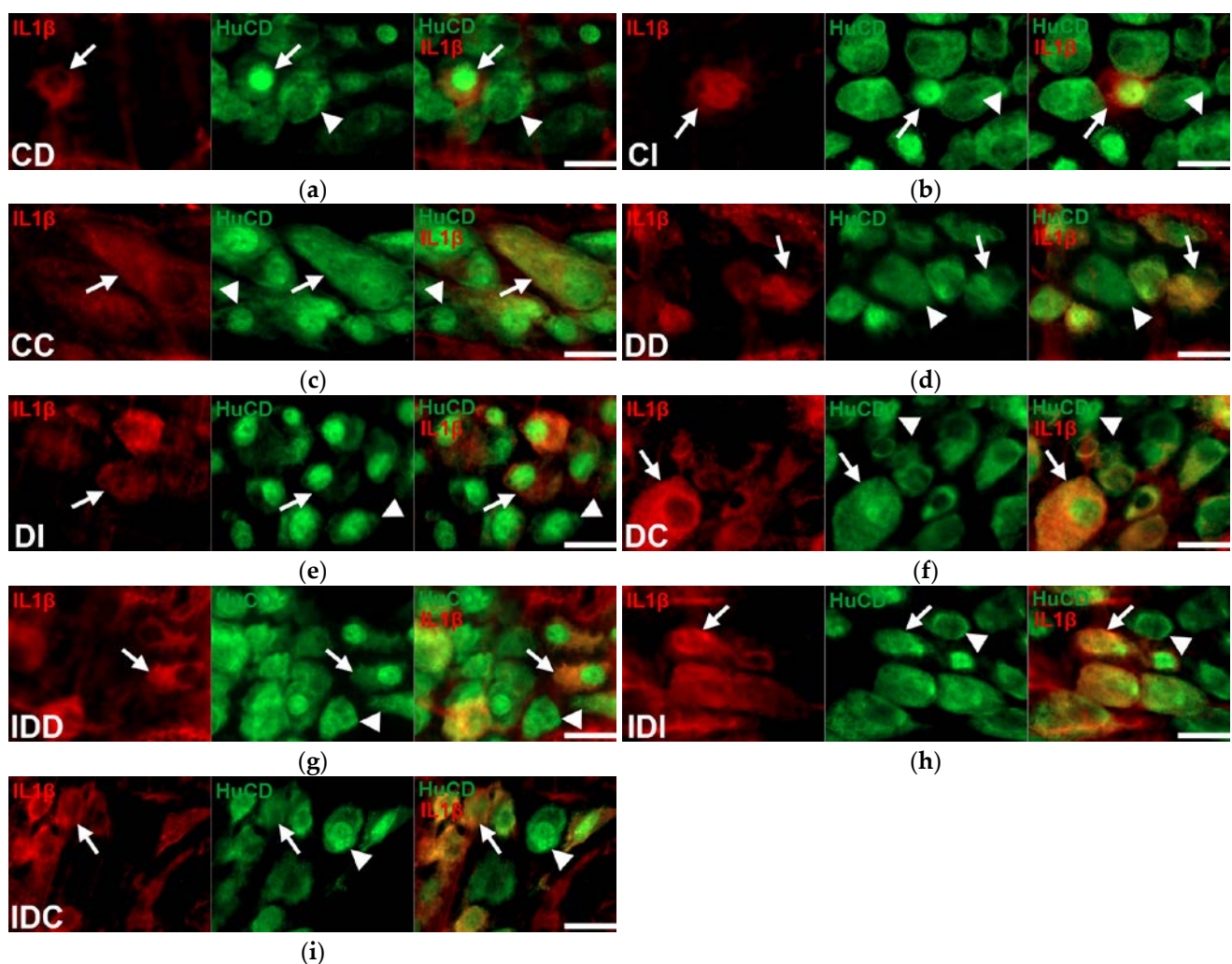


Figure 1. Representative fluorescent micrographs of whole-mount preparations of myenteric ganglia from the duodenum, ileum and colon of control, diabetic, and insulin-treated diabetic rats after IL1 β -HuC/HuD double-labelling immunohistochemistry. HuC/HuD as a pan-neuronal marker was applied to label myenteric neurons. CD—control duodenum (a), CI—control ileum (b), CC—control colon (c), DD—diabetic duodenum (d), DI—diabetic ileum (e), DC—diabetic colon (f), IDD—insulin-treated diabetic duodenum (g), IDI—insulin-treated diabetic ileum (h), IDC—insulin-treated diabetic colon (i); arrows—IL1 β -immunoreactive myenteric neurons, arrowheads—myenteric neurons. Scale bars: 20 μ m.

The proportion of IL1 β -IR myenteric neurons compared to the total myenteric neuronal number was lower in the small intestine (duodenum: $18.97 \pm 2.05\%$, ileum: $13.11 \pm 2.93\%$), than in the colonic ganglia, where it was significantly, more than 50%, higher ($50.7 \pm 4.75\%$, $p < 0.0001$) (Figure 2).

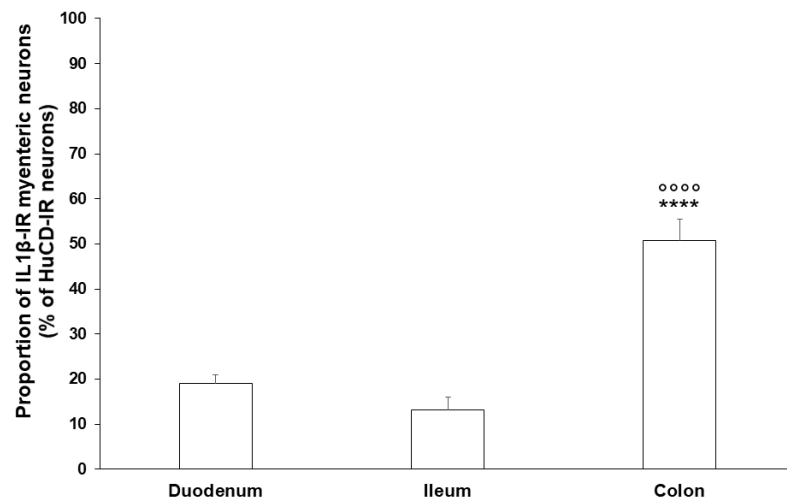


Figure 2. Proportion of IL1 β -immunoreactive myenteric neurons in the duodenum, ileum, and colon of control rats. The proportion of IL1 β -immunoreactive myenteric neurons was significantly higher in the colon compared to the ileum and duodenum. Data are expressed as mean \pm SEM. **** $p < 0.0001$ (relative to control duodenum); $^{\circ\circ\circ\circ} p < 0.0001$ (between control ileum and colon).

In diabetic rats, the IL1 β -IR myenteric neuronal proportion was significantly increased in all investigated gut segments ($p < 0.01$); it was almost doubled in the duodenum and ileum ($34.04 \pm 4.06\%$ and $24.62 \pm 3.11\%$, respectively), while it increased by more than 20% in the colon ($71.14 \pm 3.29\%$) (Figure 3). In the insulin-treated group, the proportion of IL1 β -IR myenteric neurons was not altered significantly compared to the control levels (Figure 3).

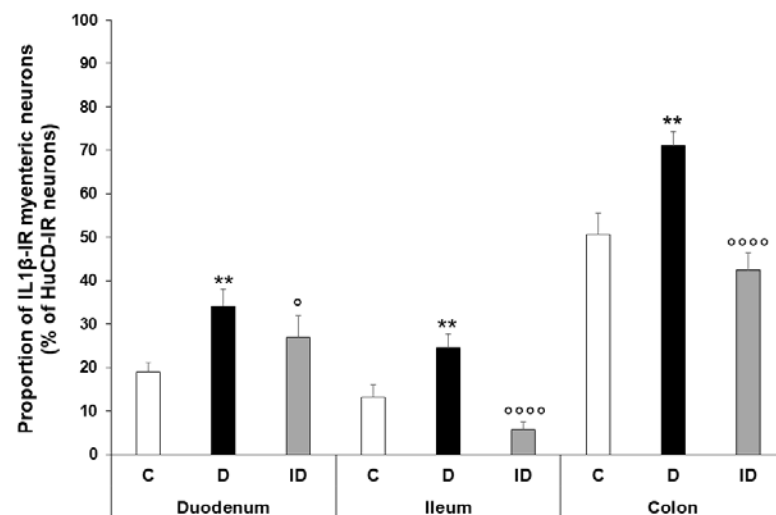


Figure 3. Proportion of IL1 β -immunoreactive myenteric neurons of the duodenum, ileum, and colon of control, diabetic and insulin-treated diabetic rats. In the diabetics, the proportion of IL1 β -immunoreactive myenteric neurons was significantly increased in all gut segments, which was prevented by immediate insulin treatment. Data are expressed as mean \pm SEM. ** $p < 0.01$ (relative to controls); $^{\circ} p < 0.05$, $^{\circ\circ\circ\circ} p < 0.0001$ (between diabetics and insulin-treated diabetics). C—controls, D—diabetics, ID—insulin-treated diabetics.

2.3. Region-Dependent Increase of IL1 β Immunoreactivity in nNOS-Immunoreactive Myenteric Neurons of Diabetic Rats

IL1 β and nNOS double-labelling immunofluorescence was applied to label IL1 β -containing nitrenergic neurons in the myenteric ganglia (Figure 4). The proportion of IL1 β -nNOS-IR cells per total nNOS-IR myenteric neurons was the lowest in the duodenum ($12.64 \pm 2.03\%$) and significantly higher in the distal segments (ileum: 36.36 ± 2.18 ; colon: 26.21 ± 2.13 ; $p < 0.0001$) of the control animals. In the diabetics, the colon was the only segment where this proportion was significantly increased ($36.94 \pm 2.76\%$ vs. $26.21 \pm 2.13\%$, $p < 0.01$), while it remained unchanged in the duodenal and ileal ganglia (Figure 5). The immediate insulin treatment did not protect against the diabetic induction of IL1 β expression in the nitrenergic neuronal population of colonic ganglia, and decreased the IL1 β -nNOS-IR neuronal proportion in the ileum (Figure 5).

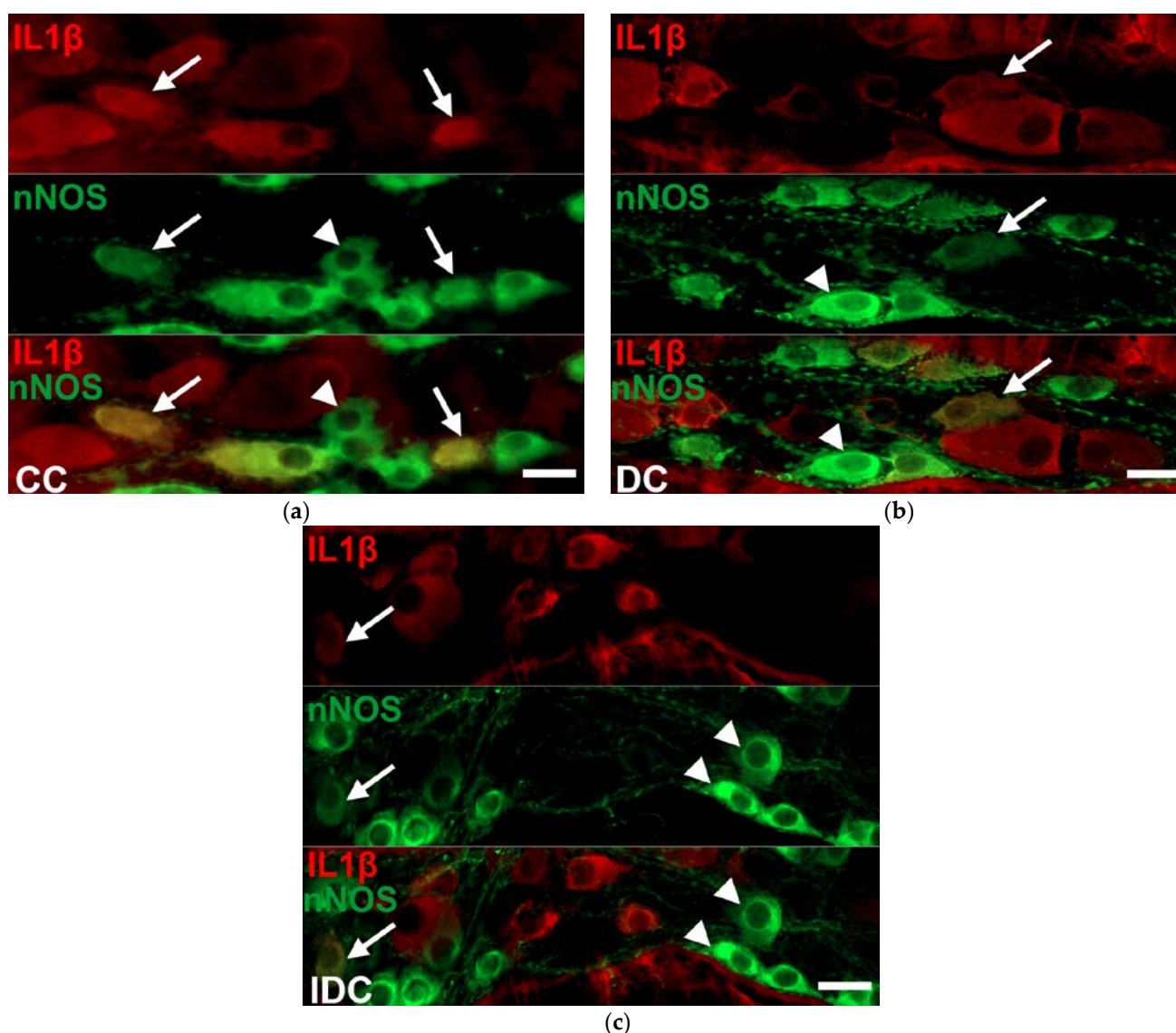


Figure 4. Representative fluorescent micrographs of whole-mount preparations of myenteric ganglia from the colon of control (a), diabetic (b), and insulin-treated diabetic (c) rats after IL1 β -nNOS double-labelling immunohistochemistry. CC—control colon, DC—diabetic colon, IDC—insulin-treated diabetic colon; arrows—IL1 β -nNOS-immunoreactive myenteric neurons, arrowheads—nNOS-immunoreactive neurons. Scale bars: 20 μ m.

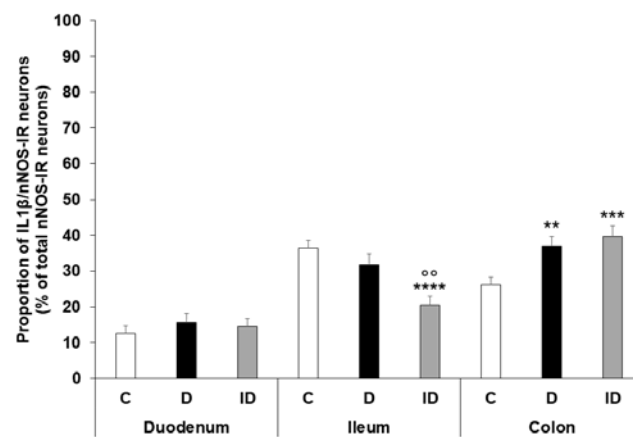


Figure 5. Proportion of IL1 β -nNOS-immunoreactive neurons related to the total number of nNOS-immunoreactive neurons in the myenteric ganglia of the duodenum, ileum, and colon of control, diabetic and insulin-treated diabetic rats. The proportion of IL1 β -nNOS-immunoreactive neurons significantly increased only in the colon of diabetics relative to controls. Data are expressed as mean \pm SEM. ** $p < 0.01$, *** $p < 0.001$, **** $p < 0.0001$ (relative to controls); °° $p < 0.01$ (between diabetics and insulin-treated diabetics). C—controls, D—diabetics, ID—insulin-treated diabetics.

2.4. Region-Dependent Increase of IL1 β Immunoreactivity in CGRP-IR Myenteric Neurons of Diabetic Rats

Myenteric neurons immunoreactivity for both IL1 β and CGRP were made visible by double-labelling fluorescent immunohistochemistry on whole-mount preparations (Figure 6).

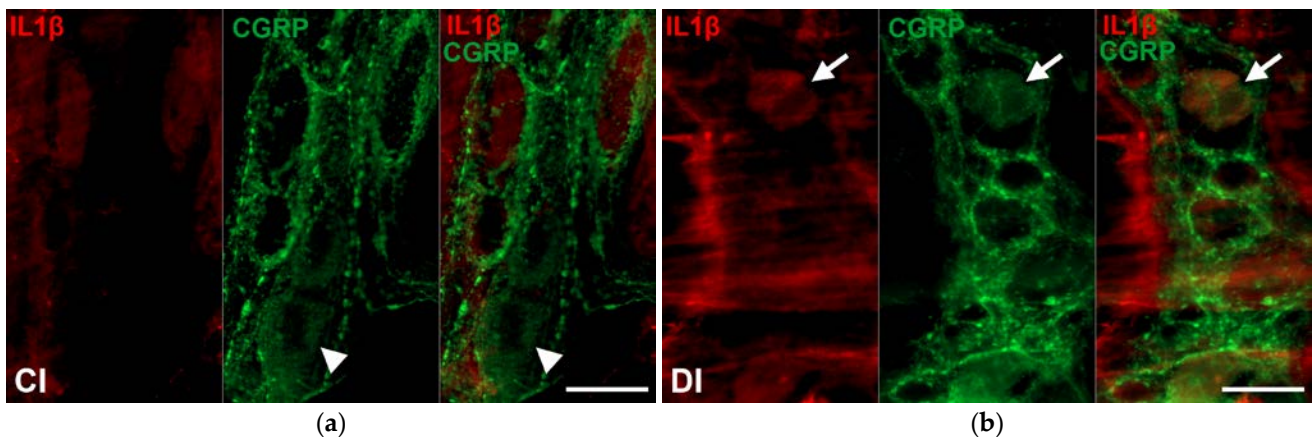


Figure 6. Representative fluorescent micrographs of whole-mount preparations of myenteric ganglia from the ileum of control (a) and diabetic (b) rats after IL1 β -CGRP double-labelling immunohistochemistry. CI—control ileum, DI—diabetic ileum; arrows—IL1 β -CGRP-immunoreactive myenteric neurons, arrowheads—CGRP-immunoreactive neurons. Scale bars: 20 μ m.

The proportion of IL1 β -CGRP-IR neurons per total CGRP-IR myenteric neurons was between 40–50% in all intestinal regions of control animals. This proportion was only significantly altered in the ileum of diabetics, where it increased compared to the controls (64.56 ± 4.17 vs. 42.13 ± 3.8 , $p < 0.01$) (Figure 7). In the insulin-treated group, an increased IL1 β -CGRP neuronal proportion was observed in the colonic ganglia compared to both controls and diabetics (Figure 7).

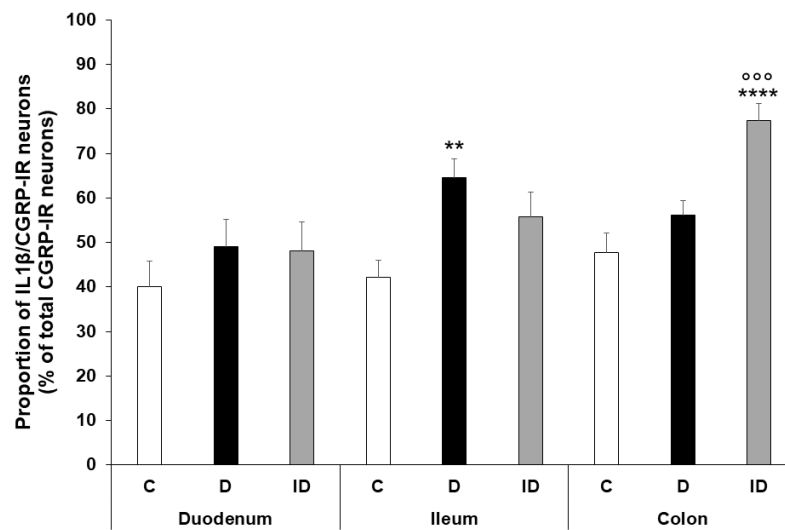


Figure 7. Proportion of IL1 β -CGRP-immunoreactive neurons related to the total number of CGRP-immunoreactive neurons in the myenteric ganglia of the duodenum, ileum, and colon of control, diabetic and insulin-treated diabetic rats. The proportion of IL1 β -CGRP-immunoreactive neurons significantly increased only in the ileum of diabetics relative to controls. Data are expressed as mean \pm SEM. ** $p < 0.01$, **** $p < 0.0001$ (relative to controls); ^{ooo} $p < 0.001$ (between diabetics and insulin-treated diabetics). C—controls, D—diabetics, ID—insulin-treated diabetics.

2.5. Increased Tissue Level of IL1 β in Colonic Muscle/Myenteric Plexus Homogenates of Diabetics

The proportion of the IL1 β -IR myenteric neurons was highest in control condition in the colon, hence the IL1 β concentration was measured here in tissue homogenates that contained the intestinal smooth muscle and the myenteric plexus. The IL1 β tissue level was 0.29 ± 0.04 ng/mg protein in control samples, while it was significantly higher in diabetic homogenates (0.94 ± 0.26 ng/mg, $p < 0.05$) and was restored to the control level in insulin-treated diabetic samples (0.4 ± 0.03 ng/mg) (Figure 8).

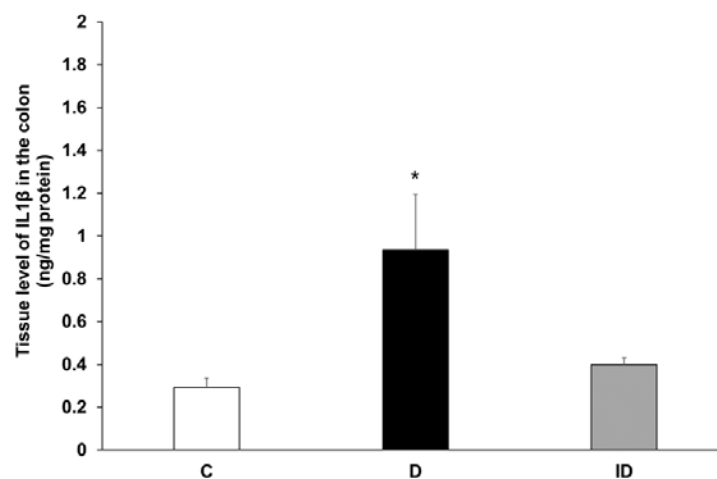


Figure 8. Tissue level of IL1 β in intestinal smooth muscle layer homogenates including the myenteric plexus from the colon of control, diabetic and insulin-treated diabetic rats. The IL1 β tissue level was significantly increased in diabetics relative to controls, which was prevented by insulin treatment. Data are expressed as means \pm SEM. * $p < 0.05$ (relative to controls). C—controls, D—diabetics, ID—insulin-treated diabetics.

2.6. Quantitative Evaluation of IL1 β mRNA Level

The IL1 β mRNA expression detected by RNAscope on cryosections in controls varied depending on the investigated gut region and intestinal layer (Figures 9 and 10).

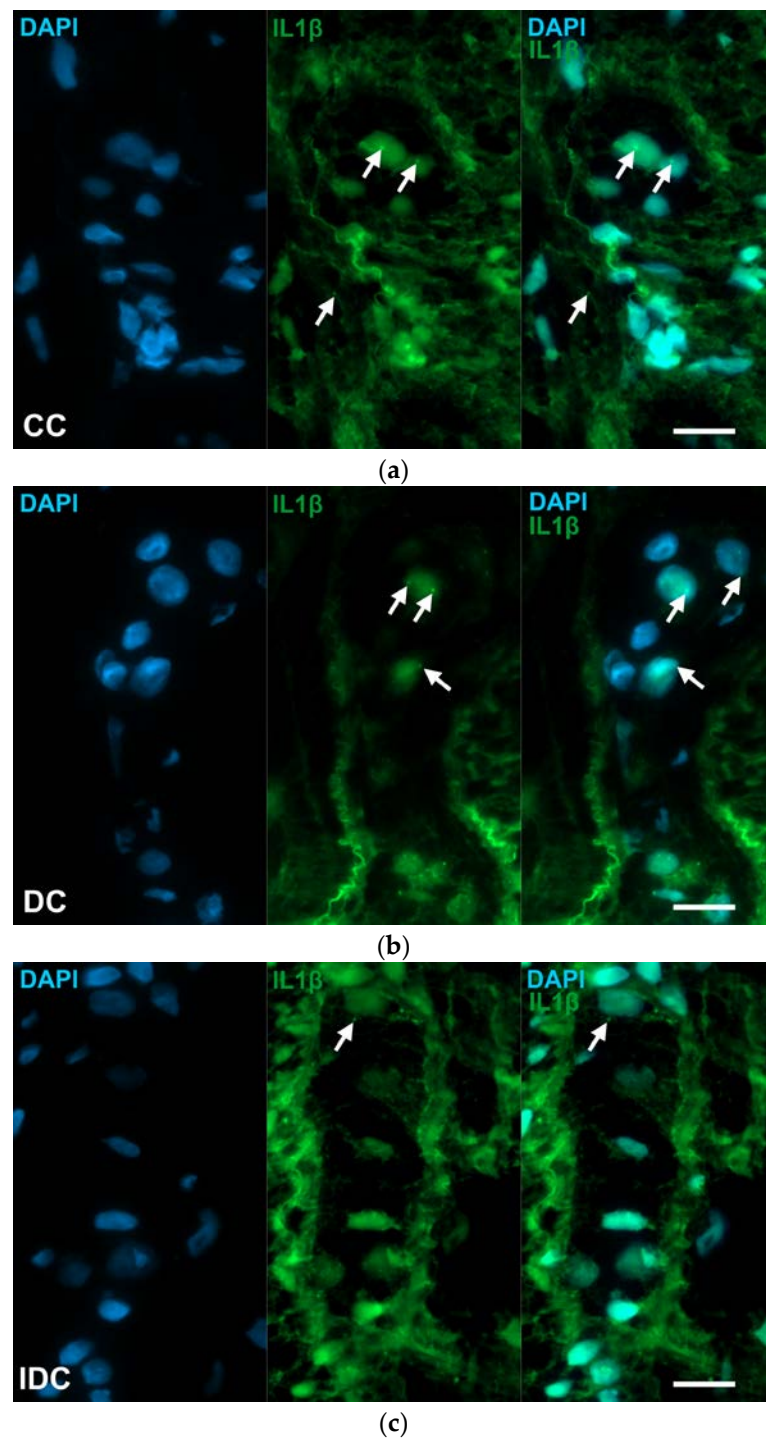


Figure 9. Representative micrographs of cryosections of myenteric ganglia from the colon of control (a), diabetic (b) and insulin-treated diabetic (c) rats after IL1 β RNAscope. IL1 β mRNA appear as green punctate dots (arrows), nuclei were counterstained with DAPI (blue). CC—control colon, DC—diabetic colon, IDC—insulin-treated diabetic colon. Scale bars: 20 μ m.

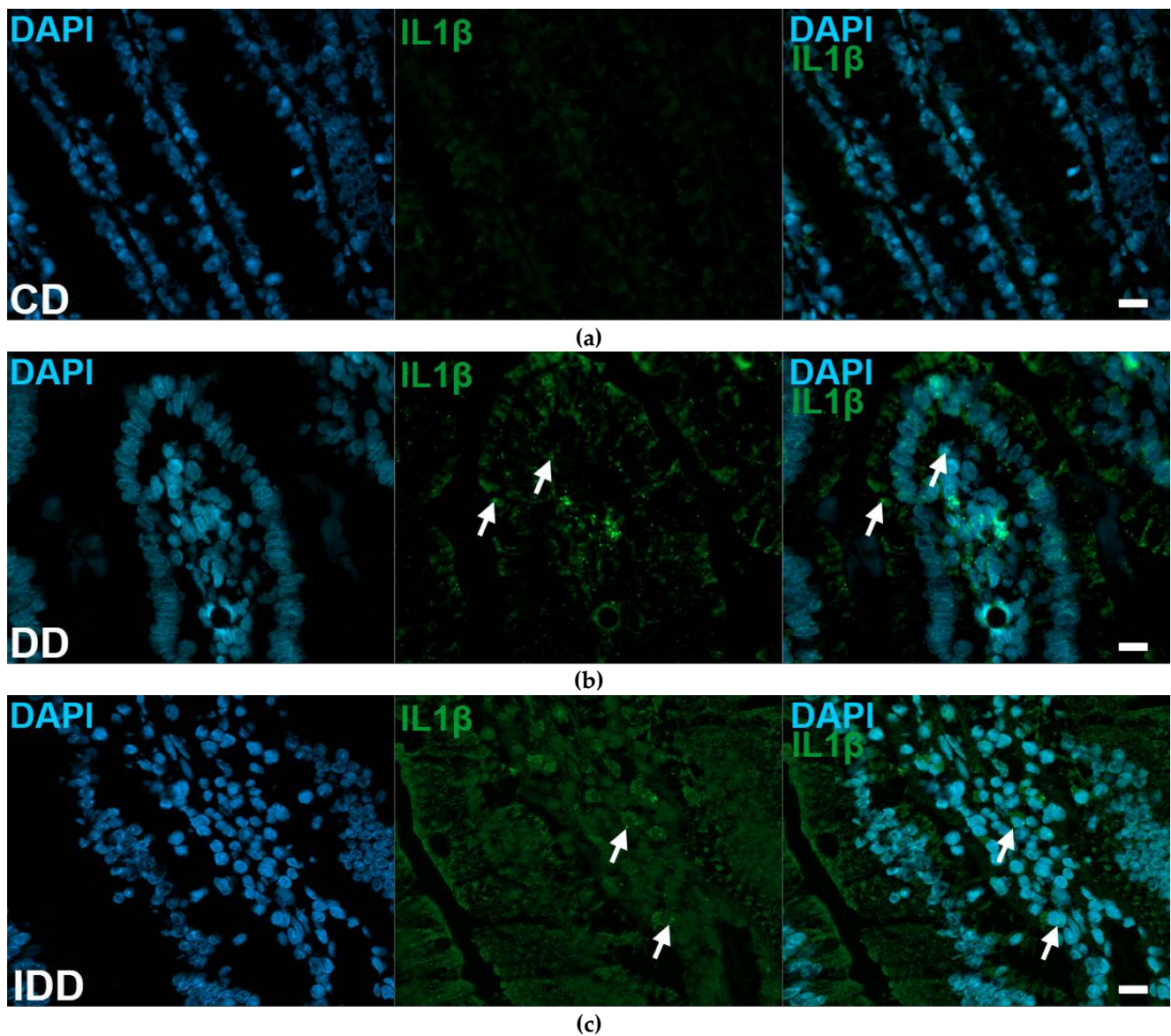


Figure 10. Representative micrographs of cryosections of mucosa from the duodenum of control (a), diabetic (b) and insulin-treated diabetic (c) rats after IL1 β RNAscope. IL1 β mRNA appear as green punctate dots (arrows), nuclei were counterstained with DAPI (blue). CD—control duodenum, DD—diabetic duodenum, IDD—insulin-treated diabetic duodenum. Scale bars: 20 μ m.

The number of punctate dots labelling IL1 β mRNA was lowest in the intestinal smooth muscle layer in all gut segments of control rats, while it was highest in the myenteric ganglia of the duodenum and colon (3400 ± 429 and 3361 ± 279.5 , respectively). In the ileum, the highest value was measured in mucosa (4558 ± 486.7), which was roughly double that of the duodenum and colon (Table 2).

Table 2. Quantitative evaluation of IL1 β mRNA labelling dots in different intestinal layers and gut segments of control rats.

	Duodenum (dots/mm ²)	Ileum (dots/mm ²)	Colon (dots/mm ²)
Myenteric ganglia	3400 \pm 429	2420 \pm 486.7	3361 \pm 279.5
Smooth muscle	1251 \pm 181.5 ^b	1629 \pm 257.7	1080 \pm 146 ^c
Mucosa	1948 \pm 281.4	4558 \pm 486.7 ^{a,e,f}	2549 \pm 279.5 ^{d,g}

Data are expressed as means \pm SEM; ^a $p < 0.05$, ^b $p < 0.001$, ^c $p < 0.0001$ vs. myenteric ganglia in the same gut segment; ^d $p < 0.01$, ^e $p < 0.001$ vs. smooth muscle in the same gut segment; ^f $p < 0.001$ vs. duodenum in the same intestinal layer; ^g $p < 0.01$ vs. ileum in the same intestinal layer.

In the myenteric ganglia of diabetic rats, the number of IL1 β mRNA labelling dots was significantly increased in all gut segments ($p < 0.05$); the greatest increase was observed in the duodenum where the dot density was almost tripled (Figure 11a). In insulin-treated diabetic rats, in the same gut region, the number of dots remained at control level (Figure 11a). In diabetics, the number of IL1 β mRNA dots increased by a lesser extent in intestinal smooth muscle as well, and this change was significant in the duodenum and colon ($p < 0.05$; Figure 11b).

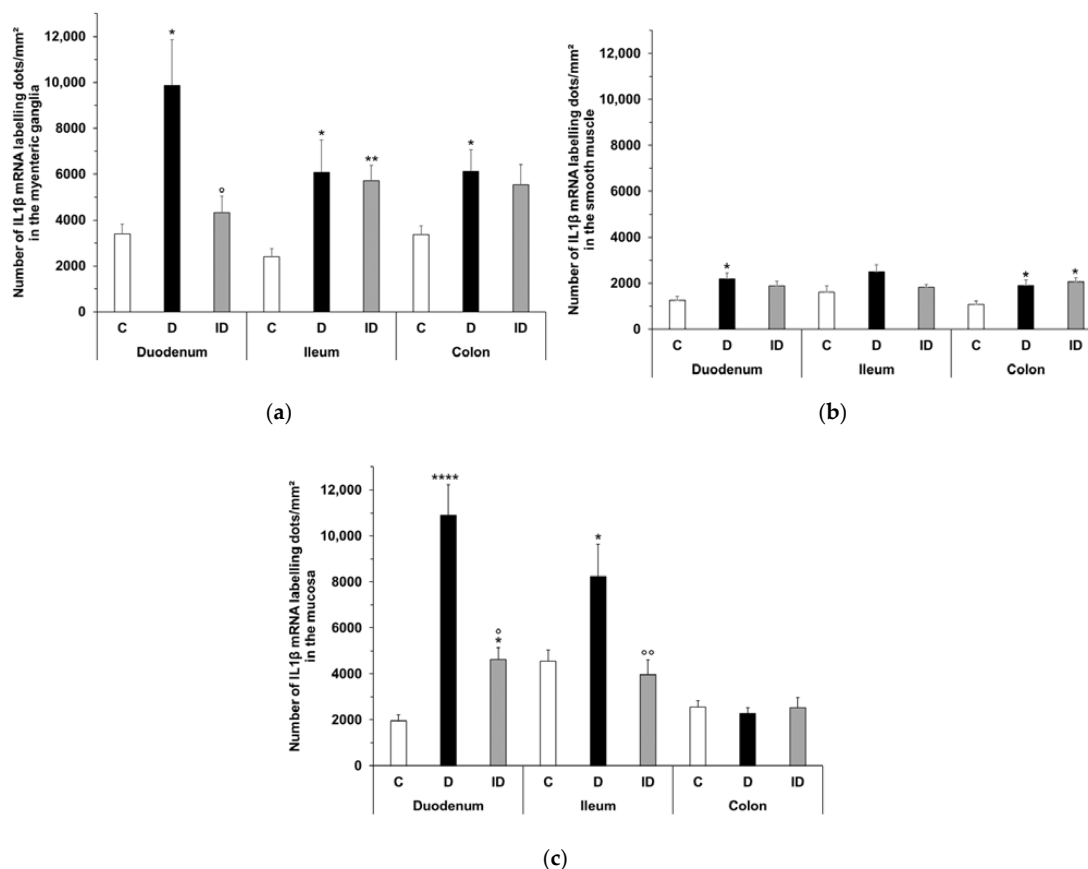


Figure 11. Expression of IL1 β mRNA in the myenteric ganglia (a), smooth muscle (b), and intestinal mucosa (c) of the duodenum, ileum, and colon of control, diabetic and insulin-treated diabetic rats. Data are expressed as mean \pm SEM. * $p < 0.05$, ** $p < 0.01$, **** $p < 0.0001$ (relative to controls); ° $p < 0.05$, °° $p < 0.01$ (between diabetics and insulin-treated diabetics). C—controls, D—diabetics, ID—insulin-treated diabetics.

In the mucosa of diabetics, IL1 β mRNA expression varied differently in different gut segments. A robust, more than five times increase in dot number was observed in the duodenum ($p < 0.0001$), and almost double in the ileum ($p < 0.05$), however, no change was

detected in the colonic mucosa (Figure 11c). Insulin treatment completely prevented the diabetic alterations in the ileum and partially in the duodenum (Figure 11c).

3. Discussion

In the present study, a distinct IL1 β induction was demonstrated in myenteric neurons in all gut segments of type 1 diabetic rats. Moreover, a strict regionality was revealed in IL1 β immunoreactivity in different myenteric subpopulations.

Although IL1 β is primarily produced by macrophages, other cell types, such as epithelial and endothelial cells, smooth muscle cells, neurons and glial cells, can also express it [20,24,42,43] and several factors can influence its release [16]. In control animals, a great difference in the proportion of IL1 β -IR myenteric neurons between the small and large intestine was observed. The high baseline level of IL1 β may be explained by an excessive pro-oxidant environment in the colon [44,45]. Similarly, other important members of the host defense and innate immunity, such as TNF α and TLR4, display higher basal distribution in the colon than in the small intestine [13,46,47].

A general induction of IL1 β expression was revealed in myenteric neurons of diabetic rats, and this induction was prevented by immediate insulin treatment. Furthermore, our observation was also confirmed in the homogenates of intestinal smooth muscle layers including the myenteric plexus prepared from the gut wall. These results reflect that the entire enteric nervous system reacts to the long-term hyperglycemic state and suggest a role for IL1 β in enteric neuroinflammation. A high glucose concentration itself can activate IL1 β precursors in different cells [48,49], which then stimulate nuclear factor kappa B activation [50], a key element of many pro-inflammatory signaling pathways. Pro-inflammatory cytokines are able to facilitate neurite growth via the upregulation of neurotrophic factors in annulus cells [51,52], cortical neural precursors [53] and myenteric neurons [25].

When investigating the nNOS-IR myenteric population in healthy controls, a higher proportion of IL1 β -containing nitrergic neurons was observed in distal gut segments, similarly to the total number of IL1 β -IR myenteric neurons. In contrast, IL1 β -containing CGRP-IR myenteric neurons exhibited an equal distribution along the duodenum–ileum–colon axis and their proportion was relatively high, 40–50%, among the total number of CGRP-IR cells. This discrepancy refers to a neuronal population-specific IL1 β expression in itself.

In diabetics, the proportion of IL1 β -containing nitrergic neurons increased only in the colonic segment, while it did not change elsewhere. Former studies [2,5] demonstrated that the nitrergic myenteric system exhibits a regional perturbation in the diabetic state, with the density of these inhibitory neurons decreasing in all intestinal segments, while this was not accompanied with neuronal loss in the duodenal ganglia. Considering these findings, it is interesting to note that, despite the nitrergic loss in the diabetic colon, the proportion of IL1 β -containing nNOS-IR neurons still increased. Other studies have shown that IL1 β is involved in the stimulation of nuclear factor κ B-mediated inducible NOS gene expression [54,55]. It has also been demonstrated that IL1 β specifically activates different neuronal and glial cell populations in the myenteric and submucous plexuses of the guinea pig ileum and colon [26]. The majority of activated myenteric neurons were nNOS-IR, while most activated submucous neurons expressed vasoactive intestinal polypeptide in both gut segments [26].

Additionally, the proportion of IL1 β -containing CGRP-IR neurons was elevated only in the ileum and remained unchanged in the duodenal and colonic ganglia of diabetics. As IPANs are essential to sense luminal stimuli, the alterations in microbial composition in diabetes may serve as a possible explanation of our results. Namely, a large-scale microbial rearrangement and robust *Klebsiella* invasion [4], together with a notable endogenous heme oxygenase defense system induction, has been detected in the ileum [2]. Several studies have demonstrated that CGRP-like immunoreactivity was decreased in both enteric plexuses of the diabetic rat ileum and colon [39,56,57], while others have observed an

increased number of CGRP-containing neurons in the pig small intestine [58]. Hou et al. showed that IL1 β can directly induce the release of CGRP from sensory neurons in a concentration-dependent manner [59]. As CGRP can modulate immune cell function, the role of neuropeptide–cytokine interactions draws attention to the importance of further investigations in diabetic enteric neuropathy [39].

At the transcriptional level, IL1 β mRNA induction was shown to occur in the myenteric ganglia in all investigated gut segments of diabetic rats and the IL1 β mRNA level was also increased in intestinal smooth muscle. The number of IL1 β mRNA-labelling dots clearly indicates that the smooth muscle of the gut wall is also a source of cytokines, although it is less affected in diabetes than the ganglia. Enhanced IL1 β mRNA expression was shown in the colonic muscle of rats with colitis [60]. Furthermore, IL1 β can induce IL6 mRNA and protein expression in cultured muscle cells of the rat jejunum [61]. The mucosal IL1 β mRNA level was robustly increased in the small intestine, especially in the duodenum of diabetics. Diabetic alterations of mucosa-associated gut microbiota [62] may induce mucosal IL1 β production [63] and contribute to an increase of intestinal permeability [9,23].

In summary, our results underline the induction of IL1 β in myenteric neurons, however, the different myenteric neuronal populations are affected in a region-dependent manner. The nNOS-IR myenteric neurons were most affected in the colon, while CGRP-IR neurons were most susceptible in the ileum of diabetic rats. Therefore, IL1 β not only determines the enteric inflammatory environment during type 1 diabetes, but may also be involved in diabetes-related alterations of enteric neurochemical phenotype, and may participate in population-specific activation of myenteric neurons leading to diabetic motility disturbances. These results may contribute to the wider use of IL1-based therapies introduced in recent years in autoinflammatory diseases [18,19,64].

4. Materials and Methods

4.1. Animal Model

Adult male Wistar rats (Toxi-Coop Zrt., Balatonfüred, Hungary) weighing 200–250 g, kept on standard laboratory chow (Innovo Kft., Zsámbék, Hungary) and with free access to drinking water, were used in the experiments. The rats were divided randomly into three groups: streptozotocin (STZ)-induced diabetics (diabetics; n = 15), insulin-treated STZ-induced diabetics (insulin-treated diabetics; n = 14), and sex- and age-matched controls (n = 16). Hyperglycemia was induced by a single intraperitoneal injection of STZ (Sigma–Aldrich, Budapest, Hungary) at 60 mg/kg [5,13,65]. The animals were considered diabetic if the non-fasting blood glucose concentration was higher than 18 mmol/L. From this time on, the insulin-treated group of hyperglycemic rats received a subcutaneous insulin injection (Humulin M3, Eli Lilly Nederland, Utrecht, The Netherlands) each morning (2 IU) and afternoon (3 IU). Equivalent volumes of saline were administered subcutaneously to the diabetic and control groups. The blood glucose levels and animal weights were measured weekly. Those diabetic animals that recovered spontaneously, or whose glucose levels decreased less than 18 mmol/L during the 10-week period, were excluded from the study. In all procedures involving experimental animals, the principles of the National Institutes of Health (Bethesda, MD, USA) guidelines and the EU directive 2010/63/EU for the protection of animals used for scientific purposes were strictly followed, and all of the experiments were approved by the National Scientific Ethical Committee on Animal Experimentation (National Competent Authority), with the license number XX./1636/2019.

4.2. Tissue Handling

Ten weeks after the onset of hyperglycemia, the animals were sacrificed by cervical dislocation under chloral hydrate anesthesia (375 mg/kg i.p.). The gut segments of diabetic, insulin-treated diabetic and control rats were dissected and rinsed in 0.05 M phosphate buffer (PB; pH 7.4). Tissue samples were taken from the duodenum (1 cm distal to the pylorus), the ileum (1 cm proximal to the ileo-cecal junction), and the proximal colon, and processed for double-labelling fluorescent immunohistochemistry, enzyme-linked

immunosorbent assay (ELISA), and RNAscope multiplex fluorescent V2 assay (RNAscope). For fluorescent immunohistochemistry, the intestinal segments were cut along the mesentery, pinched flat, and fixed overnight at 4 °C in 4% formaldehyde solution buffered with 0.1 M PB (pH 7.4). The samples were then washed, the mucosa, submucosa, and circular smooth muscle were removed, and whole-mount preparations with the myenteric plexus adhering to the longitudinal smooth muscle were prepared. For the ELISA, the 3-cm-long gut segments were cut along the mesentery and pinched flat. After removing both the mucosa and submucosa, the layers of intestinal smooth muscle including the myenteric plexus were snap-frozen in liquid nitrogen and stored at –80 °C until use. For the RNAscope, small pieces (2–3 mm) of the gut segments were fresh-frozen in liquid nitrogen, embedded in cryomatrix medium (O.C.T.TM, Tissue-Tek, Sakura, The Netherlands) and stored at –80 °C until use.

4.3. Fluorescent Immunohistochemistry

For immunofluorescence studies, IL1 β -HuC/HuD, IL1 β -nNOS or IL1 β -CGRP double-labelling immunohistochemistry were performed on whole-mounts derived from different gut segments. Briefly, after blocking in tris(hydroxymethyl)aminomethane-buffered saline (TBS) containing 1% bovine serum albumin and 10% normal goat serum, the whole-mount preparations were incubated overnight with anti-IL1 β (mouse monoclonal IgG; sc-52012, Santa Cruz Biotechnology, Dallas, TX, USA; final dilution 1:50) and pan-neuronal anti-HuC/HuD (rabbit monoclonal IgG; ab184267, Abcam, Cambridge, UK; final dilution 1:200) or anti-nNOS (rabbit polyclonal IgG; Cat. No. 160870, Cayman Chemical, Ann Arbor, MI, USA; final dilution 1:200) or anti-CGRP (rabbit polyclonal IgG; PC205L, Calbiochem, Merck, Germany; final dilution 1:100) primary antibodies at 4 °C. After washing in TBS with 0.025% Triton X-100, sections were incubated with anti-mouse CyTM3 (Jackson ImmunoResearch Laboratories, West Grove, PA, USA; final dilution 1:200) and anti-rabbit Alexa Fluor 488 (A11008, Invitrogen, Thermo Fisher Scientific, Waltham, MA, USA; final dilution 1:200) secondary antibodies for 1 h at room temperature. Negative controls were performed by omitting the primary antibodies when no immunoreactivity was observed. Whole-mounts were mounted on slides in FluoromountTM Aqueous Mounting Medium (Sigma–Aldrich, Budapest, Hungary), and observed and photographed with a Zeiss Imager Z.2 fluorescent microscope equipped with an AxioCam 506 mono camera (Zeiss, Germany, Jena). Fifty myenteric ganglia were taken from each intestinal segment from each experimental group, and the proportion of myenteric neurons that are immunoreactive for either IL1 β , IL1 β -nNOS or IL1 β -CGRP were counted per ganglia.

4.4. Measurement of Tissue IL1 β Concentration

Samples from the colon, including the intestinal smooth muscle layers with the myenteric plexus in between, were frozen in liquid nitrogen, crushed into powder in a mortar and homogenized in 500 μ L homogenizing buffer (100 μ L Protease Inhibitor Cocktail (Sigma–Aldrich, Budapest, Hungary) in 20 mL 0.05 M PB). Tissue homogenates were centrifuged at 5000 rpm for 20 min at 4 °C. The IL1 β levels of the colon samples were determined by means of quantitative ELISA according to the manufacturer's instructions (GA-E0128RT, GenAsia Biotech Co., Shanghai, China). Optical density was measured at 450 nm (Benchmark Microplate Reader; Bio-Rad, Budapest, Hungary). The tissue IL1 β concentration was expressed as ng/mg protein.

4.5. Bradford Protein Micromethod for the Determination of Tissue Protein Content

A commercial protein assay kit was used for the determination of protein content in intestinal smooth muscle/myenteric plexus homogenates of colon. Bradford reagent was added to each sample. After mixing and following 10 min incubation, the samples were assayed spectrophotometrically at 595 nm. The protein level was expressed as mg protein/mL.

4.6. RNAscope Multiplex Fluorescent V2 Assay

To detect IL1 β mRNA in different intestinal layers, the RNAscope Multiplex Fluorescent V2 Assay (Cat. No. 323100, Advanced Cell Diagnostics, Newark, CA, USA) was used according to the manufacturer's instructions. Briefly, fresh-frozen cryosections (5 μ m) were fixed in 4% formaldehyde and dehydrated in increasing ethanol concentrations. The cryosections were incubated in hydrogen peroxide, followed by protease IV treatment and then hybridized with a rat IL1 β probe (Cat. No. 314011-C2, Advanced Cell Diagnostics, Newark, CA, USA; final dilution 1:50) for 2 h at 40 °C. After a three-step signal amplification and HRP signal development combined with fluorophore (OpalTM 520 Reagent Pack, FP1487001KT, Akoya Biosciences, Menlo Park, CA, USA; final dilution 1:100, 30 min at 40 °C), tissues were counterstained with DAPI, mounted with FluoromountTM Aqueous Mounting Medium (Sigma–Aldrich, Budapest, Hungary) and photographed with a Zeiss Imager Z.2 fluorescent microscope equipped with an Axiocam 506 mono camera (Zeiss, Germany, Jena). Positive and negative control probes were also run to assess sample RNA quality and optimal permeabilization. Fifteen digital photographs of intestinal mucosa, smooth muscle and myenteric ganglia were taken from each gut segment and experimental group, and the number of punctate dots labelling IL1 β mRNA was evaluated (dots per unit area).

4.7. Statistical Analysis

A statistical analysis was performed with Kruskal–Wallis test with a Dunn's multiple comparisons test. All analyses were carried out with GraphPad Prism 6.0 (GraphPad Software, San Diego, CA, USA). A probability of $p < 0.05$ was set as the level of significance. All data are expressed as means \pm SEM.

Author Contributions: Conceptualization, M.B. and N.B.; methodology, M.B. and N.B.; validation, N.B.; investigation, A.A.D., A.E.-K., B.O., B.P.B., S.K., J.B. and Z.S.; resources, J.B. and B.P.B.; writing—original draft preparation, N.B. and M.B.; writing—review and editing, M.B. and N.B.; visualization, M.B.; supervision, M.B.; funding acquisition, N.B. All authors have read and agreed to the published version of the manuscript.

Funding: This research was funded by the Hungarian NKFIH fund project, No. FK131789 (N.B.); János Bolyai Research Scholarship of the Hungarian Academy of Sciences (N.B.), ÚNKP-22-5—New National Excellence Program of the Ministry for Innovation and Technology from the source of the National Research, Development and Innovation Fund (N.B.) and Stipendium Hungaricum Scholarship of the Tempus Public Foundation (A.A.D.).

Institutional Review Board Statement: In all procedures involving experimental animals, the principles of the National Institutes of Health (Bethesda, MD, USA) guidelines and the EU directive 2010/63/EU for the protection of animals used for scientific purposes were strictly followed, and all the experiments were approved by the National Scientific Ethical Committee on Animal Experimentation (National Competent Authority), with the license number XX./1636/2019 and Animal Welfare Committee University of Szeged with the license number I-74-11/2019 MÁB.

Informed Consent Statement: Not applicable.

Data Availability Statement: Dataset available from the corresponding author at bodi.nikolett@bio.u-szeged.hu.

Conflicts of Interest: The authors declare no conflict of interest.

References

1. Alexandraki, K.I.; Piperi, C.; Ziakas, P.D.; Apostolopoulos, N.V.; Makrilakis, K.; Syriou, V.; Diamanti-Kandarakis, E.; Kaltsas, G.; Kalofoutis, A. Cytokine secretion in long-standing diabetes mellitus type 1 and 2: Associations with low-grade systemic inflammation. *J. Clin. Immunol.* **2008**, *28*, 314–321. [[CrossRef](#)] [[PubMed](#)]
2. Chandrakumar, L.; Bagyanszki, M.; Szalai, Z.; Mezei, D.; Bodi, N. Diabetes-Related Induction of the Heme Oxygenase System and Enhanced Colocalization of Heme Oxygenase 1 and 2 with Neuronal Nitric Oxide Synthase in Myenteric Neurons of Different Intestinal Segments. *Oxid. Med. Cell. Longev.* **2017**, *2017*, 1890512. [[CrossRef](#)] [[PubMed](#)]

3. Kaiko, G.E.; Stappenbeck, T.S. Host-microbe interactions shaping the gastrointestinal environment. *Trends Immunol.* **2014**, *35*, 538–548. [[CrossRef](#)]
4. Wirth, R.; Bodi, N.; Maroti, G.; Bagyanszki, M.; Talapka, P.; Fekete, E.; Bagi, Z.; Kovacs, K.L. Regionally distinct alterations in the composition of the gut microbiota in rats with streptozotocin-induced diabetes. *PLoS ONE* **2014**, *9*, e110440. [[CrossRef](#)]
5. Izbeki, F.; Wittman, T.; Rosztoczy, A.; Linke, N.; Bodi, N.; Fekete, E.; Bagyanszki, M. Immediate insulin treatment prevents gut motility alterations and loss of nitrergic neurons in the ileum and colon of rats with streptozotocin-induced diabetes. *Diabetes Res. Clin. Pract.* **2008**, *80*, 192–198. [[CrossRef](#)]
6. Klinge, M.W.; Sutter, N.; Mark, E.B.; Haase, A.M.; Borghammer, P.; Schlageter, V.; Lund, S.; Fleischer, J.; Knudsen, K.; Drewes, A.M.; et al. Gastric Emptying Time and Volume of the Small Intestine as Objective Markers in Patients with Symptoms of Diabetic Enteropathy. *J. Neurogastroenterol. Motil.* **2021**, *27*, 390–399. [[CrossRef](#)]
7. Yarandi, S.S.; Srinivasan, S. Diabetic gastrointestinal motility disorders and the role of enteric nervous system: Current status and future directions. *Neurogastroenterol. Motil.* **2014**, *26*, 611–624. [[CrossRef](#)]
8. Caputi, V.; Popov, J.; Giron, M.C.; O'Mahony, S. Gut Microbiota as a Mediator of Host Neuro-Immune Interactions: Implications in Neuroinflammatory Disorders. *Mod. Trends Psychiatry* **2021**, *32*, 40–57. [[CrossRef](#)]
9. Al-Sadi, R.M.; Ma, T.Y. IL-1beta causes an increase in intestinal epithelial tight junction permeability. *J. Immunol.* **2007**, *178*, 4641–4649. [[CrossRef](#)]
10. Jarret, A.; Jackson, R.; Duizer, C.; Healy, M.E.; Zhao, J.; Rone, J.M.; Bielecki, P.; Sefik, E.; Roulis, M.; Rice, T.; et al. Enteric Nervous System-Derived IL-18 Orchestrates Mucosal Barrier Immunity. *Cell* **2020**, *180*, 50–63 e12. [[CrossRef](#)]
11. Ruder, B.; Atreya, R.; Becker, C. Tumour Necrosis Factor Alpha in Intestinal Homeostasis and Gut Related Diseases. *Int. J. Mol. Sci.* **2019**, *20*, 1887. [[CrossRef](#)]
12. Wei, H.X.; Wang, B.; Li, B. IL-10 and IL-22 in Mucosal Immunity: Driving Protection and Pathology. *Front. Immunol.* **2020**, *11*, 1315. [[CrossRef](#)] [[PubMed](#)]
13. Bodi, N.; Chandrakumar, L.; Al Doghmi, A.; Mezei, D.; Szalai, Z.; Barta, B.P.; Balazs, J.; Bagyanszki, M. Intestinal Region-Specific and Layer-Dependent Induction of TNFalpha in Rats with Streptozotocin-Induced Diabetes and after Insulin Replacement. *Cells* **2021**, *10*, 2410. [[CrossRef](#)] [[PubMed](#)]
14. Barta, B.P.; Onhausz, B.; Al Doghmi, A.; Szalai, Z.; Balazs, J.; Bagyanszki, M.; Bodi, N. Gut region-specific TNFR expression: TNFR2 is more affected than TNFR1 in duodenal myenteric ganglia of diabetic rats. *World J. Diabetes* **2023**, *14*, 48–61. [[CrossRef](#)]
15. McEntee, C.P.; Finlay, C.M.; Lavelle, E.C. Divergent Roles for the IL-1 Family in Gastrointestinal Homeostasis and Inflammation. *Front. Immunol.* **2019**, *10*, 1266. [[CrossRef](#)]
16. Lopez-Castejon, G.; Brough, D. Understanding the mechanism of IL-1beta secretion. *Cytokine Growth Factor Rev.* **2011**, *22*, 189–195. [[CrossRef](#)]
17. Mantovani, A.; Dinarello, C.A.; Molgora, M.; Garlanda, C. Interleukin-1 and Related Cytokines in the Regulation of Inflammation and Immunity. *Immunity* **2019**, *50*, 778–795. [[CrossRef](#)]
18. Limbert, C. Type 1 diabetes—An auto-inflammatory disease: A new concept, new therapeutical strategies. In Proceedings of the 7th European Workshop on Immune-Mediated Inflammatory Diseases, Noordwijk aan Zee, The Netherlands, 28 November 2012.
19. Broderick, L.; Hoffman, H.M. IL-1 and autoinflammatory disease: Biology, pathogenesis and therapeutic targeting. *Nat. Rev. Rheumatol.* **2022**, *18*, 448–463. [[CrossRef](#)]
20. Kaneko, N.; Kurata, M.; Yamamoto, T.; Morikawa, S.; Masumoto, J. The role of interleukin-1 in general pathology. *Inflamm. Regen.* **2019**, *39*, 12. [[CrossRef](#)]
21. Mandrup-Poulsen, T.; Pickersgill, L.; Donath, M.Y. Blockade of interleukin 1 in type 1 diabetes mellitus. *Nat. Rev. Endocrinol.* **2010**, *6*, 158–166. [[CrossRef](#)]
22. Peiro, C.; Lorenzo, O.; Carraro, R.; Sanchez-Ferrer, C.F. IL-1beta Inhibition in Cardiovascular Complications Associated to Diabetes Mellitus. *Front. Pharmacol.* **2017**, *8*, 363. [[CrossRef](#)]
23. Kaminsky, L.W.; Al-Sadi, R.; Ma, T.Y. IL-1beta and the Intestinal Epithelial Tight Junction Barrier. *Front. Immunol.* **2021**, *12*, 767456. [[CrossRef](#)] [[PubMed](#)]
24. Ren, K.; Torres, R. Role of interleukin-1beta during pain and inflammation. *Brain Res. Rev.* **2009**, *60*, 57–64. [[CrossRef](#)] [[PubMed](#)]
25. Gougeon, P.Y.; Lourenssen, S.; Han, T.Y.; Nair, D.G.; Ropeleski, M.J.; Blennerhassett, M.G. The pro-inflammatory cytokines IL-1beta and TNFalpha are neurotrophic for enteric neurons. *J. Neurosci.* **2013**, *33*, 3339–3351. [[CrossRef](#)]
26. Tjwa, E.T.; Bradley, J.M.; Keenan, C.M.; Kroese, A.B.; Sharkey, K.A. Interleukin-1beta activates specific populations of enteric neurons and enteric glia in the guinea pig ileum and colon. *Am. J. Physiol. Gastrointest. Liver Physiol.* **2003**, *285*, G1268–1276. [[CrossRef](#)]
27. Xia, Y.; Hu, H.Z.; Liu, S.; Ren, J.; Zafirov, D.H.; Wood, J.D. IL-1beta and IL-6 excite neurons and suppress nicotinic and noradrenergic neurotransmission in guinea pig enteric nervous system. *J. Clin. Investig.* **1999**, *103*, 1309–1316. [[CrossRef](#)]
28. Azpiroz, F.; Malagelada, C. Diabetic neuropathy in the gut: Pathogenesis and diagnosis. *Diabetologia* **2016**, *59*, 404–408. [[CrossRef](#)]
29. Uranga-Ocio, J.A.; Bastus-Diez, S.; Delkader-Palacios, D.; Garcia-Cristobal, N.; Leal-Garcia, M.A.; Abalo-Delgado, R. Enteric neuropathy associated to diabetes mellitus. *Rev. Esp. Enferm. Dig.* **2015**, *107*, 366–373.
30. Celtek, S. Point of NO return for nitrergic nerves in diabetes: A new insight into diabetic complications. *Curr. Pharm. Des.* **2004**, *10*, 3683–3695. [[CrossRef](#)]

31. Demedts, I.; Masaoka, T.; Kindt, S.; De Hertogh, G.; Geboes, K.; Farre, R.; Vanden Berghe, P.; Tack, J. Gastrointestinal motility changes and myenteric plexus alterations in spontaneously diabetic biobreeding rats. *J. Neurogastroenterol. Motil.* **2013**, *19*, 161–170. [[CrossRef](#)]
32. Noorian, A.R.; Taylor, G.M.; Annerino, D.M.; Greene, J.G. Neurochemical phenotypes of myenteric neurons in the rhesus monkey. *J. Comp. Neurol.* **2011**, *519*, 3387–3401. [[CrossRef](#)]
33. Qu, Z.D.; Thacker, M.; Castellucci, P.; Bagyanszki, M.; Epstein, M.L.; Furness, J.B. Immunohistochemical analysis of neuron types in the mouse small intestine. *Cell Tissue Res.* **2008**, *334*, 147–161. [[CrossRef](#)]
34. Bodi, N.; Szalai, Z.; Bagyanszki, M. Nitrergic Enteric Neurons in Health and Disease-Focus on Animal Models. *Int. J. Mol. Sci.* **2019**, *20*, 2003. [[CrossRef](#)]
35. Boyer, L.; Sidpra, D.; Jevon, G.; Buchan, A.M.; Jacobson, K. Differential responses of VIPergic and nitrergic neurons in paediatric patients with Crohn's disease. *Auton. Neurosci.* **2007**, *134*, 106–114. [[CrossRef](#)] [[PubMed](#)]
36. Burlinski, P.J.; Rychlik, A.; Calka, J. Effects of inflammation and axotomy on expression of acetylcholine transferase and nitric oxide synthetase within the cocaine- and amphetamine-regulated transcript-immunoreactive neurons of the porcine descending colon. *J. Comp. Pathol.* **2014**, *150*, 287–296. [[CrossRef](#)]
37. Furness, J.B.; Jones, C.; Nurgali, K.; Clerc, N. Intrinsic primary afferent neurons and nerve circuits within the intestine. *Prog. Neurobiol.* **2004**, *72*, 143–164. [[CrossRef](#)]
38. Hibberd, T.J.; Yew, W.P.; Dodds, K.N.; Xie, Z.; Travis, L.; Brookes, S.J.; Costa, M.; Hu, H.; Spencer, N.J. Quantification of CGRP-immunoreactive myenteric neurons in mouse colon. *J. Comp. Neurol.* **2022**, *530*, 3209–3225. [[CrossRef](#)] [[PubMed](#)]
39. Chandrasekharan, B.; Srinivasan, S. Diabetes and the enteric nervous system. *Neurogastroenterol. Motil.* **2007**, *19*, 951–960. [[CrossRef](#)] [[PubMed](#)]
40. Domenech, A.; Pasquinelli, G.; De Giorgio, R.; Gori, A.; Bosch, F.; Pumarola, M.; Jimenez, M. Morphofunctional changes underlying intestinal dysmotility in diabetic RIP-I/hIFNbeta transgenic mice. *Int. J. Exp. Pathol.* **2011**, *92*, 400–412. [[CrossRef](#)]
41. Zandecki, M.; Vanden Berghe, P.; Depoortere, I.; Geboes, K.; Peeters, T.; Janssens, J.; Tack, J. Characterization of myenteric neuropathy in the jejunum of spontaneously diabetic BB-rats. *Neurogastroenterol. Motil.* **2008**, *20*, 818–828. [[CrossRef](#)]
42. Copray, J.C.; Mantingh, I.; Brouwer, N.; Biber, K.; Kust, B.M.; Liem, R.S.; Huitinga, I.; Tilders, F.J.; Van Dam, A.M.; Boddeke, H.W. Expression of interleukin-1 beta in rat dorsal root ganglia. *J. Neuroimmunol.* **2001**, *118*, 203–211. [[CrossRef](#)]
43. Guo, W.; Wang, H.; Watanabe, M.; Shimizu, K.; Zou, S.; LaGraize, S.C.; Wei, F.; Dubner, R.; Ren, K. Glial-cytokine-neuronal interactions underlying the mechanisms of persistent pain. *J. Neurosci.* **2007**, *27*, 6006–6018. [[CrossRef](#)] [[PubMed](#)]
44. Brown, H.; Esterhazy, D. Intestinal immune compartmentalization: Implications of tissue specific determinants in health and disease. *Mucosal Immunol.* **2021**, *14*, 1259–1270. [[CrossRef](#)]
45. Sanders, L.M.; Henderson, C.E.; Hong, M.Y.; Barhoumi, R.; Burghardt, R.C.; Carroll, R.J.; Turner, N.D.; Chapkin, R.S.; Lupton, J.R. Pro-oxidant environment of the colon compared to the small intestine may contribute to greater cancer susceptibility. *Cancer Lett.* **2004**, *208*, 155–161. [[CrossRef](#)] [[PubMed](#)]
46. Bodi, N.; Egyed-Kolumban, A.; Onhausz, B.; Barta, B.P.; Doghmi, A.A.; Balazs, J.; Szalai, Z.; Bagyanszki, M. Intestinal Region-Dependent Alterations of Toll-Like Receptor 4 Expression in Myenteric Neurons of Type 1 Diabetic Rats. *Biomedicines* **2023**, *11*, 129. [[CrossRef](#)]
47. Price, A.E.; Shamardani, K.; Lugo, K.A.; Deguine, J.; Roberts, A.W.; Lee, B.L.; Barton, G.M. A Map of Toll-like Receptor Expression in the Intestinal Epithelium Reveals Distinct Spatial, Cell Type-Specific, and Temporal Patterns. *Immunity* **2018**, *49*, 560–575 e566. [[CrossRef](#)] [[PubMed](#)]
48. Honma, K.; Machida, C.; Mochizuki, K.; Goda, T. Glucose and TNF enhance expression of TNF and IL1B, and histone H3 acetylation and K4/K36 methylation, in juvenile macrophage cells. *Gene* **2020**, *763S*, 100034. [[CrossRef](#)] [[PubMed](#)]
49. Maedler, K.; Sergeev, P.; Ris, F.; Oberholzer, J.; Joller-Jemelka, H.I.; Spinass, G.A.; Kaiser, N.; Halban, P.A.; Donath, M.Y. Glucose-induced beta cell production of IL-1beta contributes to glucotoxicity in human pancreatic islets. *J. Clin. Investig.* **2002**, *110*, 851–860. [[CrossRef](#)]
50. Flodstrom, M.; Welsh, N.; Eizirik, D.L. Cytokines activate the nuclear factor kappa B (NF-kappa B) and induce nitric oxide production in human pancreatic islets. *FEBS Lett.* **1996**, *385*, 4–6. [[CrossRef](#)]
51. Gruber, H.E.; Hoelscher, G.L.; Bethea, S.; Hanley, E.N., Jr. Interleukin 1-beta upregulates brain-derived neurotrophic factor, neurotrophin 3 and neuropilin 2 gene expression and NGF production in annulus cells. *Biotech. Histochem.* **2012**, *87*, 506–511. [[CrossRef](#)]
52. Gruber, H.E.; Jones, B.; Marrero, E.; Hanley, E.N., Jr. Proinflammatory Cytokines IL-1beta and TNF-alpha Influence Human Annulus Cell Signaling Cues for Neurite Growth: In Vitro Coculture Studies. *Spine* **2017**, *42*, 1529–1537. [[CrossRef](#)]
53. Park, S.Y.; Kang, M.J.; Han, J.S. Interleukin-1 beta promotes neuronal differentiation through the Wnt5a/RhoA/JNK pathway in cortical neural precursor cells. *Mol. Brain* **2018**, *11*, 39. [[CrossRef](#)] [[PubMed](#)]
54. Cho, J.M.; Chang, S.Y.; Kim, D.B.; Needs, P.W.; Jo, Y.H.; Kim, M.J. Effects of physiological quercetin metabolites on interleukin-1beta-induced inducible NOS expression. *J. Nutr. Biochem.* **2012**, *23*, 1394–1402. [[CrossRef](#)]
55. Kim, M.J.; Ryu, G.R.; Kang, J.H.; Sim, S.S.; Min, D.S.; Rhie, D.J.; Yoon, S.H.; Hahn, S.J.; Jeong, I.K.; Hong, K.J.; et al. Inhibitory effects of epicatechin on interleukin-1beta-induced inducible nitric oxide synthase expression in RINm5F cells and rat pancreatic islets by down-regulation of NF-kappaB activation. *Biochem. Pharmacol.* **2004**, *68*, 1775–1785. [[CrossRef](#)]

56. Shotton, H.R.; Broadbent, S.; Lincoln, J. Prevention and partial reversal of diabetes-induced changes in enteric nerves of the rat ileum by combined treatment with alpha-lipoic acid and evening primrose oil. *Auton. Neurosci.* **2004**, *111*, 57–65. [[CrossRef](#)]
57. Spangeus, A.; Suhr, O.; El-Salhy, M. Diabetic state affects the innervation of gut in an animal model of human type 1 diabetes. *Histol. Histopathol.* **2000**, *15*, 739–744. [[CrossRef](#)] [[PubMed](#)]
58. Bulc, M.; Calka, J.; Palus, K. Effect of Streptozotocin-Induced Diabetes on the Pathophysiology of Enteric Neurons in the Small Intestine Based on the Porcine Diabetes Model. *Int. J. Mol. Sci.* **2020**, *21*, 2047. [[CrossRef](#)] [[PubMed](#)]
59. Hou, L.; Li, W.; Wang, X. Mechanism of interleukin-1 beta-induced calcitonin gene-related peptide production from dorsal root ganglion neurons of neonatal rats. *J. Neurosci. Res.* **2003**, *73*, 188–197. [[CrossRef](#)] [[PubMed](#)]
60. Khan, I.; al-Awadi, F.M. Colonic muscle enhances the production of interleukin-1 beta messenger RNA in experimental colitis. *Gut* **1997**, *40*, 307–312. [[CrossRef](#)] [[PubMed](#)]
61. Khan, I.; Blennerhassett, M.G.; Kataeva, G.V.; Collins, S.M. Interleukin 1 beta induces the expression of interleukin 6 in rat intestinal smooth muscle cells. *Gastroenterology* **1995**, *108*, 1720–1728. [[CrossRef](#)]
62. Wirth, R.; Bódi, N.; Szalai, Z.; Chandrakumar, L.; Maróti, G.; Kovács, L.K.; Bagi, Z.; Mezei, D.; Balázs, J.; Bagyánszki, M. Perturbation of the mucosa-associated anaerobic gut microbiota in streptozotocin-induced diabetic rats. *Acta Biol. Szeged.* **2021**, *65*, 75–84. [[CrossRef](#)]
63. Benedetti, F.; Curreli, S.; Zella, D. Mycoplasmas-Host Interaction: Mechanisms of Inflammation and Association with Cellular Transformation. *Microorganisms* **2020**, *8*, 1351. [[CrossRef](#)]
64. Dinarello, C.A. Blocking interleukin-1beta in acute and chronic autoinflammatory diseases. *J. Intern. Med.* **2011**, *269*, 16–28. [[CrossRef](#)] [[PubMed](#)]
65. Jancso, Z.; Bodi, N.; Borsos, B.; Fekete, E.; Hermes, E. Gut region-specific accumulation of reactive oxygen species leads to regionally distinct activation of antioxidant and apoptotic marker molecules in rats with STZ-induced diabetes. *Int. J. Biochem. Cell Biol.* **2015**, *62*, 125–131. [[CrossRef](#)] [[PubMed](#)]

Disclaimer/Publisher's Note: The statements, opinions and data contained in all publications are solely those of the individual author(s) and contributor(s) and not of MDPI and/or the editor(s). MDPI and/or the editor(s) disclaim responsibility for any injury to people or property resulting from any ideas, methods, instructions or products referred to in the content.